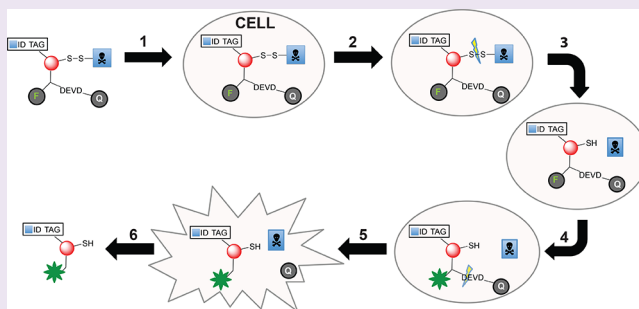


Toward a Microparticle-Based System for Pooled Assays of Small Molecules in Cellular Contexts

Carrie E. Yozwiak,[†] Tal Hirschhorn,[‡] and Brent R. Stockwell^{*,†,‡,§}[†]Department of Chemistry, Columbia University, New York, New York 10027, United States[‡]Department of Biological Sciences, Columbia University, Northwest Corner Building, MC 4846, 550 West 120th Street, New York, New York 10027, United States**S** Supporting Information

ABSTRACT: Experimental approaches to the discovery of small molecule probes and drug candidates often use biochemical or cell-based screening of large libraries ($>10^5$) of small molecules. Small molecules of interest are tested one at a time in individual wells of a microtiter plate, at a significant cost in time and resources. Furthermore, evaluation of large numbers of compounds in such assays requires robust cellular or biochemical screening formats that may not be relevant to the contexts found in human patients. We envision a solution to these issues that involves a pooled system of small molecule screening, which would require development of numerous new technologies, and solutions to several key challenges. We report here that a microparticle-based screening system can allow for screening of small molecules in such a pooled fashion, analogous to the pooled screens of genetic reagents that have been powerfully deployed in recent years. We developed a cleavable linker that can link small molecules of interest to silica microparticle beads, a DNA tag encoding the identity of the small molecule on each bead that was attached to the silica beads through a photocleavable linker to enable its amplification, and a bead-based fluorescent sensor that can report on the activity of small molecules in cells. We suggest that this pooled small molecule screening system could ultimately be useful for drug and probe discovery, allowing rapid and inexpensive screening of small molecules in assays of relevance to human diseases.



Therapeutic small molecule candidates often fail upon exposure to the complex physiology found in animal models and human patients, which are not captured in simple high-throughput tissue culture screening systems. In addition, the time and expense needed to assess the effects of large numbers of small molecules limits the number of compounds that can be tested and requires significant resources.

This problem of evaluating large numbers of reagents in physiologically relevant cell and animal models has been addressed for genetic reagents such as RNAi,¹ CRISPR,² and cDNA,³ by creating barcoded retroviral libraries that can be used to infect target cells in culture or in animal models. Using these tools, effective reagents can be selected and decoded using a rapid and inexpensive procedure compared to testing of individual reagents one at a time in an arrayed fashion. In order to more efficiently analyze biological activities of small molecules, a pooled approach would similarly be useful. Large scale pooling of small molecules is not possible, because all cells are exposed to each compound, creating uninterpretable effects of large mixtures of compounds. This problem was solved for genetic reagents by physically packaging each test reagent into separate viral particles, which can deliver one genetic reagent to each infected cell, when the multiplicity of infection (MOI) is suitably calibrated.

Pooling has thus emerged as a powerful approach to efficiently perform genetic screens. For example, pooled RNAi barcode screens provide a convenient method to evaluate large shRNA libraries. In this method, shRNA vectors are tagged with a unique oligonucleotide sequence before infection of cells and then analyzed *via* PCR amplification and barcode sequencing. The understanding of gene function acquired by large-scale pooled RNAi screens has greatly contributed to the understanding of cell signaling and drug target discovery for cancer and infectious diseases.^{4–6} In addition, such pooled barcode shRNA screens have been performed both in cell culture assays and in animal models.^{7,8}

There is no pooled small molecule screening method for cellular assays that is analogous to pooled, genetic screening technology. A major limiting factor is that multiple small molecules can penetrate cells. The current paradigm is therefore a one-compound-in-one-well approach, which provides a straightforward analysis, at the cost of being relatively inefficient and expensive to screen large small molecule libraries without substantial automation.⁹ Moreover,

Received: January 13, 2018

Accepted: January 24, 2018

Published: January 24, 2018

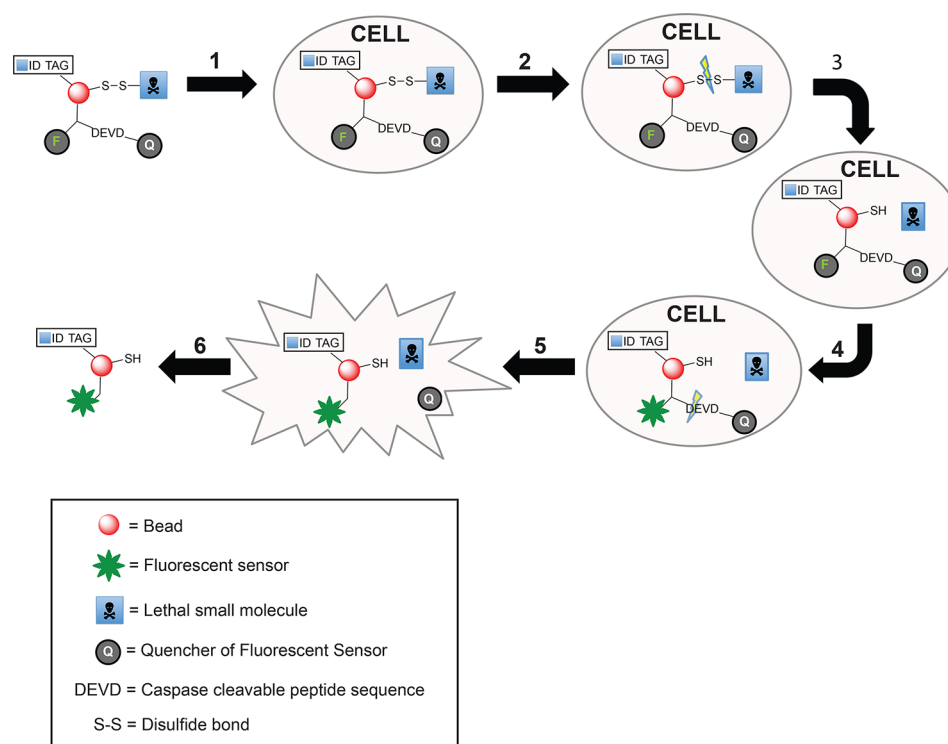


Figure 1. Design of bead-based system for pooled screening of small molecules. (1) The technology, containing the covalently bound small molecule, identification tag, and activity reporter, is internalized by the cell. (2) Once inside the cell, the small molecule is released through the reduction of the disulfide bond linker.²³ The small molecule exists inside the cell without chemical modification. (4) If the small molecule causes apoptosis, activated caspases will cleave the DEVD peptide sequence bridging FRET pair. (5) Loss of FRET results in increased fluorescence on the bead. (6) The activated system will be sorted based on this change in fluorescence, and the barcode sequenced to identify the small molecule that caused cell lethality. Red bead, silica microparticle; S-S, disulfide linker; blue square, lethal small molecule; Q, quencher; F, fluorescent dye.

evaluating the effects of individual compounds in animal models requires great time, expense, and large numbers of animals.

Merrifield's revolutionary development of solid-phase peptide synthesis set the stage for technologies that generate large libraries of diverse peptides and small molecules.¹⁰ Split-pool synthesis methods rely on chemical conjugation of peptides or small molecules to a resin in a one-bead–one-compound (OBOC) format. After the initial coupling reaction is performed on different aliquots of beads, the beads are pooled and resplit, and a new chemical moiety is added to each group of beads. This cycle of split-pool synthesis is repeated to efficiently generate large libraries of structurally diverse compounds for screening.^{11–13} Screening of these compound-bead libraries has been demonstrated in isolated protein systems, but not in intact cells, because cells generally do not internalize the synthesis beads used for split-pool synthesis.^{14,15}

Herein, we report several advances that enable the development of a technology for pooled small molecule screening in cellular assays. Using fluorescent silica microparticle beads coated with carboxylate groups, we covalently attached three components to the bead surface—(1) small molecules to be assayed *via* a cleavable linker, (2) a fluorescent reporter, and (3) a photocleavable barcode encoding the identity of each test small molecule. We examined the utility of each aspect of this system in proof of concept experiments in human tumor cell culture models.

RESULTS

We designed a microparticle-bead-based system that could deliver small molecules into cells and report on the identity of the small molecule tested and its cellular activity (Figure 1). Once taken up into cells, the beads were designed to release each test small molecule either by disulfide bond cleavage or cleavage of a linker peptide by cellular proteases. We envisioned that a fluorescent reporter would indicate if the small molecule delivered to a particular cell was exerting the biological activity of interest. For example, if a small molecule initiates apoptosis, executioner caspase 3 would be activated. Caspase 3 cleaves the DEVD amino acid sequence,¹⁶ other fluorescent peptide reporters could similarly report on the activity of other proteases in cells. A fluorescent reporter attached to beads was thus designed to detect caspase 3 activation; it consists of a fluorescence resonance energy transfer (FRET) pair¹⁷ separated by a DEVD peptide sequence. Once apoptosis occurs as a result of exposure of the cells to the released small molecule, activated caspase 3 cleaves the DEVD sequence, resulting in a loss of FRET. The increase in the fluorescence intensity of the donor fluorophore can be detected by flow cytometry, and the bead can then be separated from beads in which the FRET signal persists. Finally, a cleavable oligonucleotide barcode attached to the beads can be amplified using PCR and then sequenced, to identify the small molecule that caused caspase activation in the cellular context being tested (Supporting Information Figure 1).

We reasoned that during the course of a pooled small molecule screen, the beads must be harvested in order to sequence barcodes that encode the identity of the test

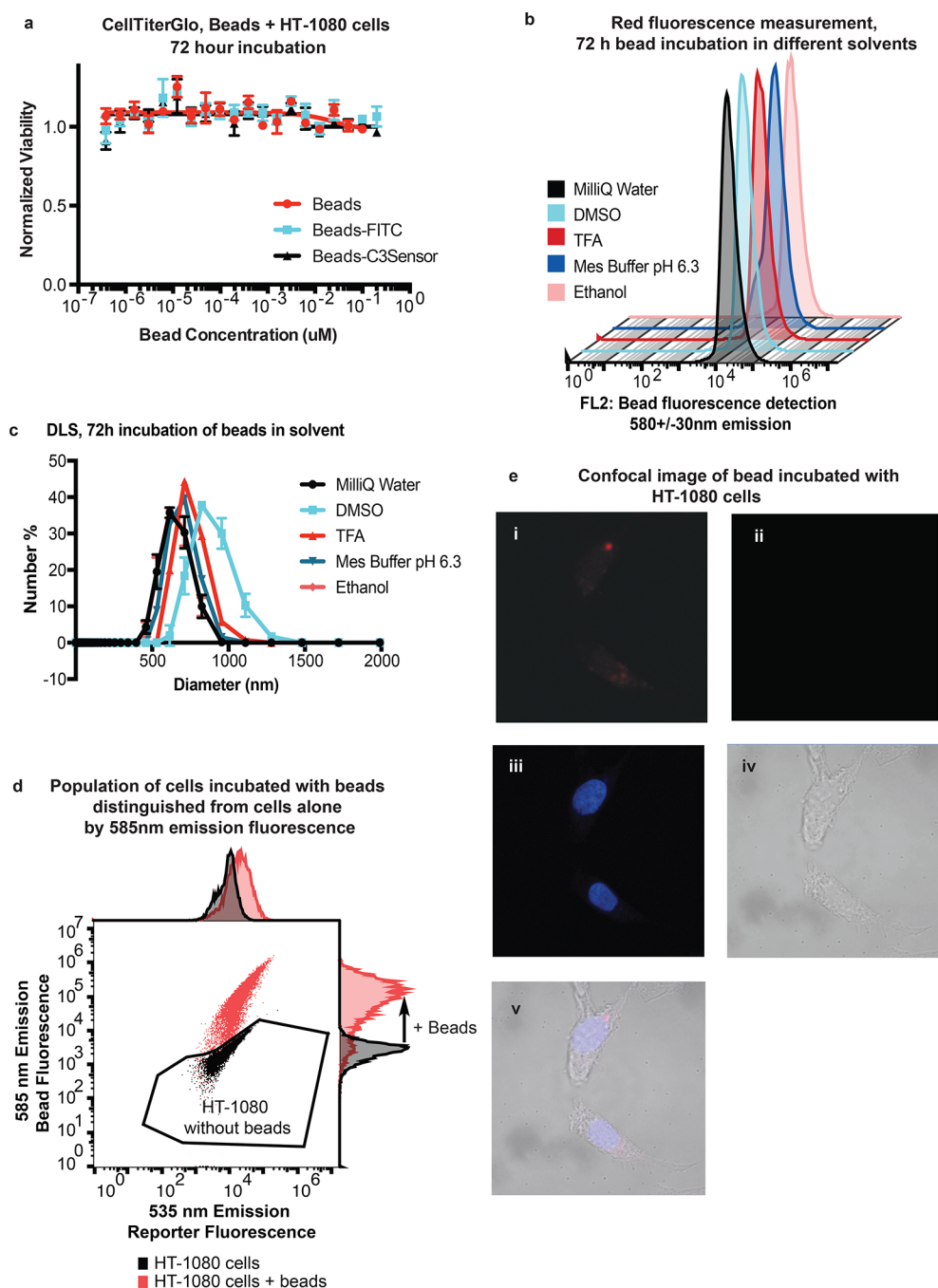


Figure 2. Selection of 1 μm silica bead for technology transport vehicle. (a) Cell viability of red beads after 72 h incubation with HT-1080 cells shows no lethality. (b) Flow cytometry data of beads show diverse solvents do not alter bead fluorescence detected on the 585/40 nm emission detection (FL2) channel. (c) Dynamic light scattering (DLS) analysis of beads after 72 h incubation with diverse solvents shows no bead degradation. (d) Scatter plot of flow cytometry data. A gate of the live cell population before bead incubation was applied, and 10 000 events for each trial were recorded inside the gate. A total of $92 \pm 0.40\%$ of HT-1080 cells incubated with a 1 μm diameter bead showed a 99-fold average increase in 585/40 nm filter (FL2 detectable fluorescence) over the control population after 6 h. (e) Confocal Z-stack image of HT-1080 cells incubated for 6 h with 1 μm diameter silica beads shows microparticle uptake. (i) Red bandpass filter shows fluorescent bead. (ii) Green bandpass filter shows no bead bleedthrough. (iii) Transmitted light. (iv) DAPI. (v) Overlay.

compounds attached to each bead. The beads must thus be made of a material that does not affect cell viability, and that does not decompose upon cellular internalization or cell lysis. Cell viability experiments with varying concentrations of 1 μm silica microparticles showed no lethality after incubation for 72 h (Figure 2a), suggesting these beads are suitable, based on these criteria.

Microparticle fluorescence and structure were maintained after incubation in dimethyl sulfoxide (DMSO), dimethylformamide (DMF), ethanol, water, and 2-(*N*-morpholino)ethanesulfonic acid (MES) solvents, suggesting that silica beads are compatible with a variety of organic synthesis conditions, in contrast to other solid-phase microparticle materials we examined. Regardless of the solvent environment, the fluorescence intensity of the beads at the appropriate emission

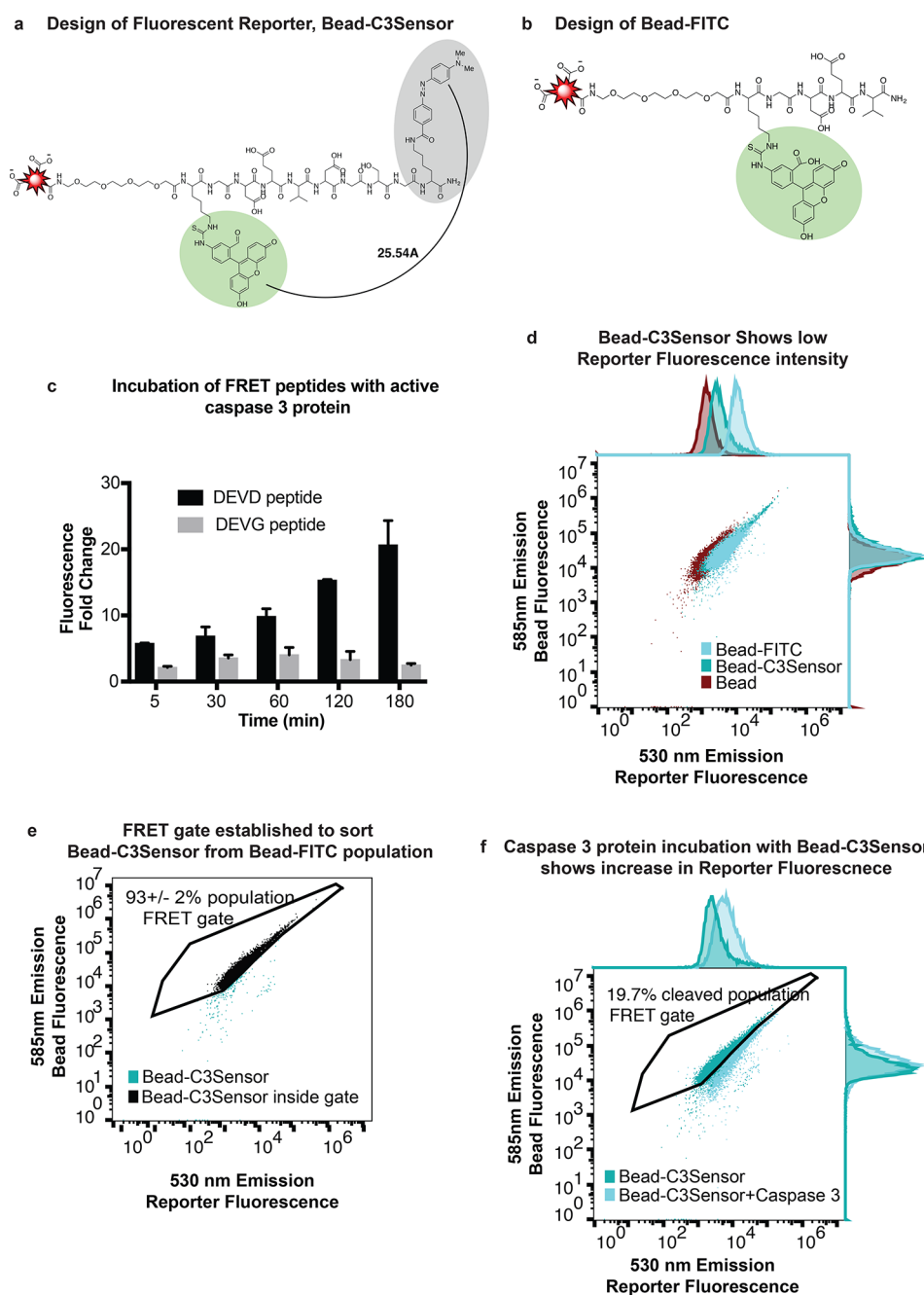


Figure 3. Design and activity analysis of fluorescent reporter component. (a) Design of FRET-based reporter conjugated to the bead, which we refer to as “Bead-C3Sensor.” Upon caspase 3 exposure, the DEVD sequence is cleaved after the aspartic acid to release the dabcyil quencher. FITC fluorescence increases, resulting from the distance-dependent loss of FRET. (b) Design of the Bead-FITC system, used as a control for cell intake studies and flow cytometry analysis. (c–e) Biochemical assay to assess FRET efficiency. (c) Flow cytometry data of the bead without peptide (red), the bead conjugated to FRET peptide, Bead-C3Sensor (dark blue), and the bead conjugated to the FITC peptide, Bead-FITC (light blue). A total of 10 000 events were recorded for seven different samples of each population. The bead emission detection signal (y axis) stayed consistent between all populations, demonstrating the bead fluorescence was not altered. The reporter emission detection channel (x axis) registers the FITC signal and was quenched upon dabcyil addition. F test between FITC and FRET populations on the reporter emission detection channel = 0.26 ($n = 7$). (d) The FRET gate for FACS sorting. A gate²⁸ was included to encompass $93 \pm 1.8\%$ of the Bead-C3Sensor population ($n = 8$). (e) The FRET gate²⁸ is applied to the Bead-C3Sensor after 3 h of incubation with active Caspase-3 protein. On average, the gate overlaps with $30 \pm 7.0\%$ of the population ($n = 10$). The remainder of the sample (blue) will be harvested for barcode sequencing. On average, we can expect to sequence 70% of the lethal small molecule population. Overlay of the Bead-C3Sensor system with the Bead-C3Sensor + caspase 3 incubation shows a detectable difference in reporter fluorescence emission channel.

detection channel of a flow cytometer remained constant (Figure 2b).

Dynamic light scattering (DLS) was used to analyze the microparticle size distribution profile of beads (Figure 2c). DLS

measurements assess the scattering of a monochromatic light source by particles in a solution; the similar size distribution of each group of beads demonstrated bead stability across diverse solvents. Additionally, we found that the carboxylate function-

ality on these beads was compatible with bioconjugation reactions with oligonucleotides and peptides.

We thus envisioned that silica particles would act as the delivery vehicle for the system. Given the robust solvent stability of silica microparticles and their compatibility with diverse synthetic organic chemistry reaction conditions, we next examined the biocompatibility and size requirements of this material. We realized that the beads must be small enough to be internalized by cells, yet must possess a sufficient concentration of synthetic handles to conjugate a suitable amount of each component onto the bead. Our goal was to find a bead type that demonstrates sufficient cellular uptake with a maximum of functional handles for chemical synthesis. To evaluate the appropriate balance of these factors, we studied cellular uptake of fluorescent microparticles that were 1 μm in diameter in HT-1080 fibrosarcoma cells. Because the beads possess a fluorescence emission maximum at 625 nm, cells that internalized the beads showed an increase in fluorescence on the FL2 channel of the flow cytometer, which detects a fluorescence emission of 585/40 nm (Figure 2d). The fluorescence of 10 000 live HT-1080 cells without beads ($n = 4$) was examined as a control to develop a suitable gate on the bead emission detection channel of the flow cytometer versus the fluorescence emission of the reporter component (FITC, excitation 488 nm, emission recorded on 585 nm channel) such that the gate encompassed $99.8 \pm 0.2\%$ of the population. The gate was applied to each sample and was used to discriminate between cells without beads versus cells with fluorescent beads. Of the live cell population analyzed, $8.2 \pm 0.4\%$ of cells did not take up a 1 μm bead after 6 h of incubation ($n = 3$); this population did not show an increase in fluorescence intensity on the 585 nm channel, the bead emission fluorescence channel. We found that smaller beads were taken up by virtually all cells, but the surface area available and fluorescence intensity on smaller beads were less favorable for compound delivery (Supporting Information Figure 2a). Confocal microscopy confirmed cellular internalization of these 1 μm diameter beads (Figure 2e); thus, we determined that this size would be ideal for maximizing the available microparticle surface, while still being amenable to cell uptake. By adapting the multiplicity of infection concept from viral screening, we were able to deliver a single bead into individual cells (Supporting Information Figure 2b). The 1 μm silica beads were internalized by multiple different human cancer derived cell lines (Supporting Information Figure 2c), suggesting these beads would be suitable for examining biological activity in a variety of contexts.

A FRET sensor can act as a reporter of protease activity, to allow for selection of compounds that induce specific protease activity.¹⁸ The integrity of the FRET pair should be maintained in live cells and disrupted upon activation of a protease to yield a detectable change in fluorescence. We evaluated this concept initially with small molecules that cause cell death through caspase-dependent apoptosis, a well-defined mechanism of cell death with biomarkers available for reliable detection.¹⁹ Additionally, the evasion of apoptosis is a hallmark of cancer, so discovering small molecules that initiate apoptosis might be therapeutically relevant; indeed, venetoclax, an inhibitor of Bcl-2 proteins that induces apoptosis, has recently been approved for clinical use by the U.S. FDA.²⁰

Caspase 3 is the main executioner enzyme in apoptosis.^{21,22} This cysteine protease specifically cleaves after the peptide sequence DEVD.^{16,22} For effective fluorescence quenching, FRET relies on three principles: (1) overlap between the

emission spectrum of the donor fluorophore and the excitation spectra of the acceptor fluorophore, (2) a donor–acceptor pair distance of 1–10 nm, and²³ (3) suitable orientation of the FRET pair for effective nonradiative, resonance transfer of energy.²⁴ Because FRET is a distance-dependent effect, we placed the DEVD substrate between the FRET pair to create “C3sensor” (Figure 3a). Upon caspase 3 activation, the peptide should be cleaved, to increase the distance from the donor fluorophore (FITC) to the acceptor chromophore (dabcyl). FRET pair separation should result in increased fluorescence signal of the FITC dye (Figure 3b). Indeed, we found that the fluorescence intensity of FITC increased 15-fold when incubated with 0.5 units of purified active caspase 3 protein for 2 h (Figure 3c).

The FRET-caspase sensor was conjugated to silica microparticles by an amide linkage *via* 1-ethyl-3-(3-(dimethylamino)propyl)carbodiimide (EDC) coupling of the primary amino terminus to the carboxylate-bead coating. We designated this covalently linked reporter–bead complex as “Bead-C3Sensor.” To ensure that the peptide was covalently bound to the bead, we analyzed the zeta potential of the microparticles. Zeta potential measurements assess the electrostatic potential of the surface of particles suspended in aqueous solution by tracking the movement of charged particles across an applied electric field.²⁵ Similarly charged particles in solution correlate to a large zeta potential and demonstrate stable colloidal dispersion and low agglomeration of the suspension. After conjugation, the zeta potential increased, demonstrating less repulsion between particles and thus supporting effective conjugation (Supporting Information Figure 3a). To examine cellular internalization of the microparticle-peptide system, a peptide labeled with fluorescent FITC without the dabcyl quencher was used as a control (Figure 3b). The FITC-only containing peptide is equivalent to the cleaved product of the bead with the FRET pair exposed to caspase 3, and shows high fluorescent intensity at two emission peaks corresponding to both the bead and the dye (Figure 3d). This peptide fluorescence would be equivalent to 100% protease efficiency in cleaving each conjugated DEVD sequence. Fluorescence measurements demonstrated covalent attachment of the FITC-peptide to the bead (Supporting Information Figure 3b), and confocal microscopy showed internalization of the peptide-bead system, Bead-FITC (Figure 5a).

We recognized that it is essential to distinguish the fluorescent reporter in the quenched FRET pair on beads from beads exposed to active caspase 3, so that flow cytometry can effectively separate each population. Ineffective separation would result in a high degree of false-positives. Flow cytometry analysis of the Bead-C3Sensor conjugated pair showed comparable FITC fluorescence intensity to the bead alone (Figure 3d). Both of these populations were distinct from the bead-FITC conjugated pair, which showed a distinct increase in fluorescence intensity on the reporter fluorescence detection channel (Figure 3d). After the Bead-C3Sensor was exposed to purified, active caspase 3 protein, there was a distinct shift to higher reporter emission fluorescence intensity when compared to the original, uncleaved FRET state (Figure 3f). When a gate that encompasses $93 \pm 2\%$ of the native Bead-C3Sensor system (Figure 3e) was applied to the Bead-C3Sensor exposed to active caspase 3 protein, $70 \pm 7\%$ of the beads have increased reporter fluorescence sufficient to fall outside of the gate (Figure 3f). That population is the target for harvesting, and the

barcode of those samples could be sequenced to identify apoptosis-inducing small molecules.

Furthermore, we tested whether a fluorescent reporter could be designed to specifically sense the activity of other proteases in a cellular context. We thus replaced the caspase-sensitive, DEVD peptide motif in the Bead-C3Sensor with a cathepsin D cleavable motif (bead-CatSensor). Cathepsin D is a lysosomal aspartic endopeptidase localized in intracellular structures, such as endosomes, lysosomes, or phagosomes; as such, it should colocalize with the bead system if the beads are internalized by endocytosis.

We reasoned that cathepsin D access to the bead–sensor system would cleave the peptide motif, separate the FRET pair, and increase sensor fluorescence. Indeed, we found that HT-1080 cells containing the bead-CatSensor exhibited a 3.6-fold increase in sensor fluorescence over cells containing the bead control (Supporting Information Figure 3c). Additionally, the Bead-CatSensor system exhibited a 70% increase in fluorescence intensity in HT-1080 cells compared to cells treated with chloroquine, which should suppress lysosomal cathepsin D activity. Finally, we detected a 1.5-fold increase in fluorescence intensity in cells with this sensor compared to cells pretreated with the cathepsin inhibitor Pepstatin A, suggesting that we were reporting on cathepsin protease activity. Together, these experiments suggest that it is possible to design protease sensors that report on different protease activities in cells, particularly in the lysosomal compartment where the beads get taken up.

Next, we recognized that each barcode must be uniquely matched to each small molecule tested, show no bias in PCR amplification, stay covalently bound to the bead throughout the assay, and be sequenced to reveal a statistical distribution of “hits.” We developed oligonucleotide barcodes consisting of 45 unique base pair sequences flanked by forward and reverse primer regions (Supporting Information Table S2). Each distinct barcode sequence used the same set of primers, so multiple “hit” small molecules out of the pool could be equally amplified and identified. The primer design includes an overhang region with a sequence compatible with existing DNA sequencing technology.

Prototype DNA barcodes were synthesized and attached to beads through an amide linkage after reaction with a terminal primary amine on the 5' end. In addition, a photocleavable linker was included in the barcode design (Figure 4a), which we found necessary for acceptable PCR efficiency. Upon irradiation with near-UV light (300–350 nm range to avoid DNA damage), cleavage of the DNA from the bead was observed after 10 min (Figure 4b). This cleavable linker was included to make PCR amplification of the oligonucleotide more efficient after isolation of the bead, as we found that PCR amplification was inefficient on beads: lack of amplification was observed when the oligonucleotide remained bound to the bead and can likely be explained by steric hindrance of the bead to the polymerase. The bulky bead may block the polymerase from binding to the oligonucleotide, preventing DNA extension.

Two unique barcodes were initially used for a proof of principle to ensure effective primer binding to more than one sequence (Figure 4b). Once the barcode was conjugated to the bead, the system was incubated for 24 h with the lysate of cells that were undergoing apoptosis. Despite protease activation and other environmental changes that occur during the programmed death pathway, the oligonucleotide was effectively PCR amplified after photocleavage from the bead (Figure 4c).

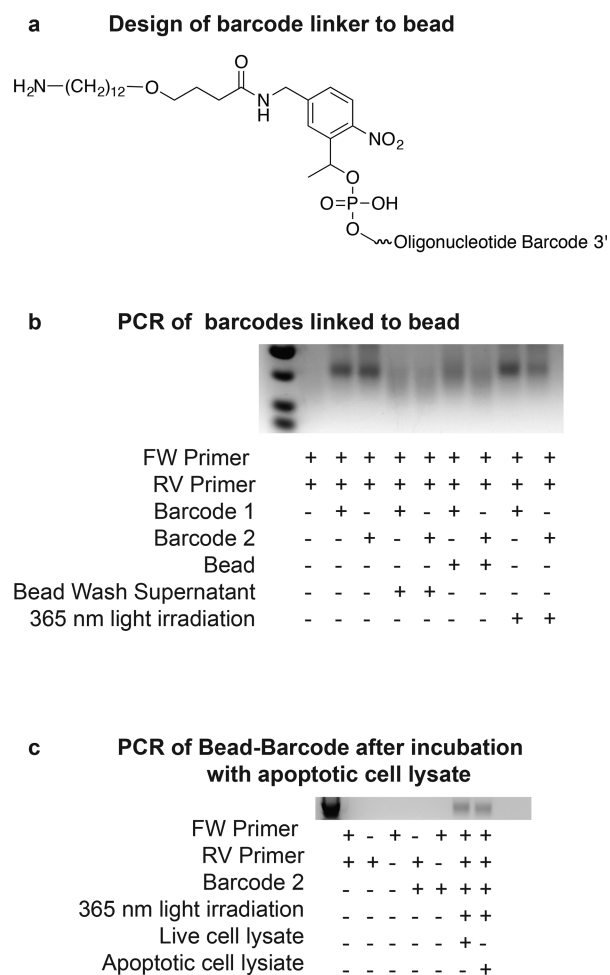


Figure 4. Small molecule identification tag, design, and amplification. (a) Design of barcode component. (b) Electrophoresis DNA gel after PCR amplification of the barcode. The photocleavable linker was necessary for adequate amplification. Using similar thermocycler conditions and identical primers, barcodes of different sequences were amplified with similar efficiency. There is no bias observed for one sequence over the other. (c) Electrophoresis DNA gel after PCR amplification of the barcodes incubated with cell lysate. A band at the appropriate molecular weight marker is observed, demonstrating that the oligonucleotide sequence is maintained throughout lysis conditions and exposure to enzymes and cellular components present during cell death by apoptosis.

This suggests the bead–barcode conjugated pair can persist throughout the entirety of the screen for small molecule identification, a key feature of a pooled small molecule screening system.

To evaluate the compatibility of the sensor and the barcode, both were covalently coupled to the bead by a one-pot EDC coupling, as confirmed by zeta potential measurements. The addition of the oligonucleotide to the bead–peptide conjugate made the zeta potential slightly more negative (Supporting Information Figure 3a). Additionally, dynamic light scattering showed an increase in particle size upon barcode attachment (Supporting Information Figure 4). Confocal microscopy showed internalization of this bead–dye–oligo reagent (Figure 5a and b) and that this was not lethal to HT-1080 cells after 48 h of incubation (Figure 5c).

An additional key component of the small molecule pooled screening technology needed is covalent attachment of test

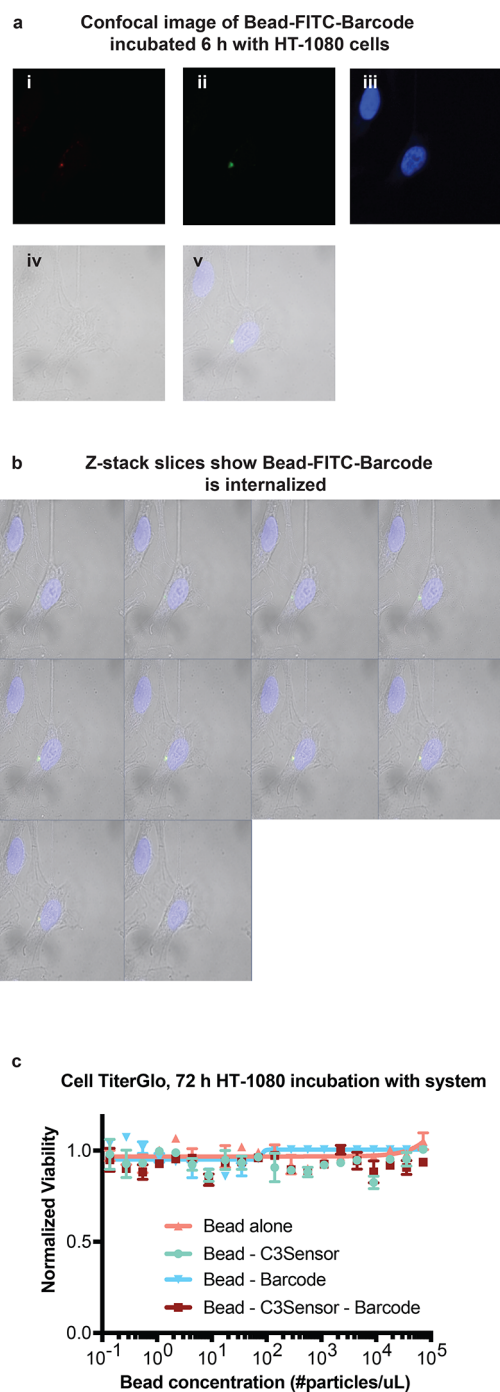


Figure 5. Bead-FITC-barcode internalization by HT-1080 cells. (a) Confocal microscopy internal slice of Z-stack image, after Bead-FITC-Barcode technology incubation with HT-1080 cells for 6 h. (i) Bead fluorescence in red bandpass filter. (ii) FITC fluorescence of FITC-peptide conjugated to bead in green bandpass filter. (iii) Transmitted light. (iv) DAPI. (v) Overlay. (vi) Full Z-stack overlay image. (b) Slices of Z-stack produced by confocal microscopy of Bead-FITC-Barcode technology with HT-1080 incubation. Yellow overlay shows colocalization of Bead-FITC signal. Outermost slices show no bead presence, supporting the observation that the cell internalizes the bead. (c) HT-1080 cells incubated for 72 h with varying concentrations of bead conjugated to the barcode and fluorescent reporter show no decrease in cell viability.

small molecules. The small molecules of interest should detach from the bead only once the system is internalized into cells.

We first examined the utility of the potentially glutathione-reductase-rich environment of the cytosol to employ a disulfide-bond linker to connect the bead to the small molecule (Supporting Information Figure 5). Although a covalent bond is maintained outside of the cellular environment, once internalized, the disulfide bond should be reduced to cleave the small molecule from the cell. Once inside the cell, the small molecule should not contain any additional chemical modifications that can alter its biological activity. The lethal small molecule used for this proof of concept experiment was the microtubule inhibitor mertansine (DM1). DM1 was chosen because of its potency (4.6 nM in HT-1080 cells) to induce apoptosis (Supporting Information Figure 6b). Additionally, DM1 possesses a terminal thiol moiety in its active state, thus simplifying the model by eliminating the need for a self-immolative linker. The chemistry used to covalently attach the known lethal molecule is outlined in Supporting Information Scheme 1.

The first step of integrating the components of the system involves differentiating a portion of the surface of the bead with a functionality to react with the small molecule. We sought a high concentration of each small molecule to be bound to each bead, to maximize the ultimate cellular concentration achieved. When using 0.5 equiv of mono-Boc protected diamine per one equivalent of carboxylate group on the bead surface, there is a large enough concentration of unreacted carboxylate handles on the bead for effective conjugation and detection of the barcode and fluorescent reporter, but the majority of chemical space on the bead surface will be unreactive to these moieties, having been coupled to the protected diamine. It is thus inert to the subsequent EDC couplings and reserved for small molecule attachment. Deprotection of the Boc moiety to reveal a primary amine was possible with concentrated trifluoroacetic acid because the silica bead withstands strong acid and the more sensitive groups (peptide, oligonucleotide) are not yet attached (Supporting Information Figure 1). Facile coupling of 3-(2-pyridylthio)propionic acid *N*-hydroxysuccinimide ester (SPDP) to the newly differentiated bead surface yields a pyridine-disulfide moiety that withstands the chemistry to attach the oligo and fluorophore, yet will react during a simple and robust thiol-sulfide exchange reaction to attach the lethal small molecule to the bead in the last step (Figure 6a). On the basis of the average cell diameter (20 μm), the reaction efficiency, and the number of carboxylate groups per bead, we have calculated the average cellular concentration of the small molecule to be $\sim 100 \mu\text{M}$, which is more than sufficient to identify promising compounds out of a first-pass screen, even if overall loading and release efficiency is low. On the basis of the coupling equivalents, this could be tuned to lower concentrations for more stringent assays.

To test the actual release of active small molecules in cells, we synthesized a noncleavable linker using maleimide bioconjugation chemistry to control for disulfide bond reduction and release of the small molecule after bead uptake (Figure 6b). We did not detect apoptosis with either cleavable or noncleavable small molecule–bead conjugated system, suggesting cellular reductases could not release the compound from the disulfide linker; this suggests that the beads do not get released from the lysosome into the cytosol.

We thus evaluated the cathepsin D cleavable linker, which should release compounds from endosomal compartments when the bead system encounters cathepsin D. We conjugated the lethal molecule monomethyl auristatin E (MMAE) to beads

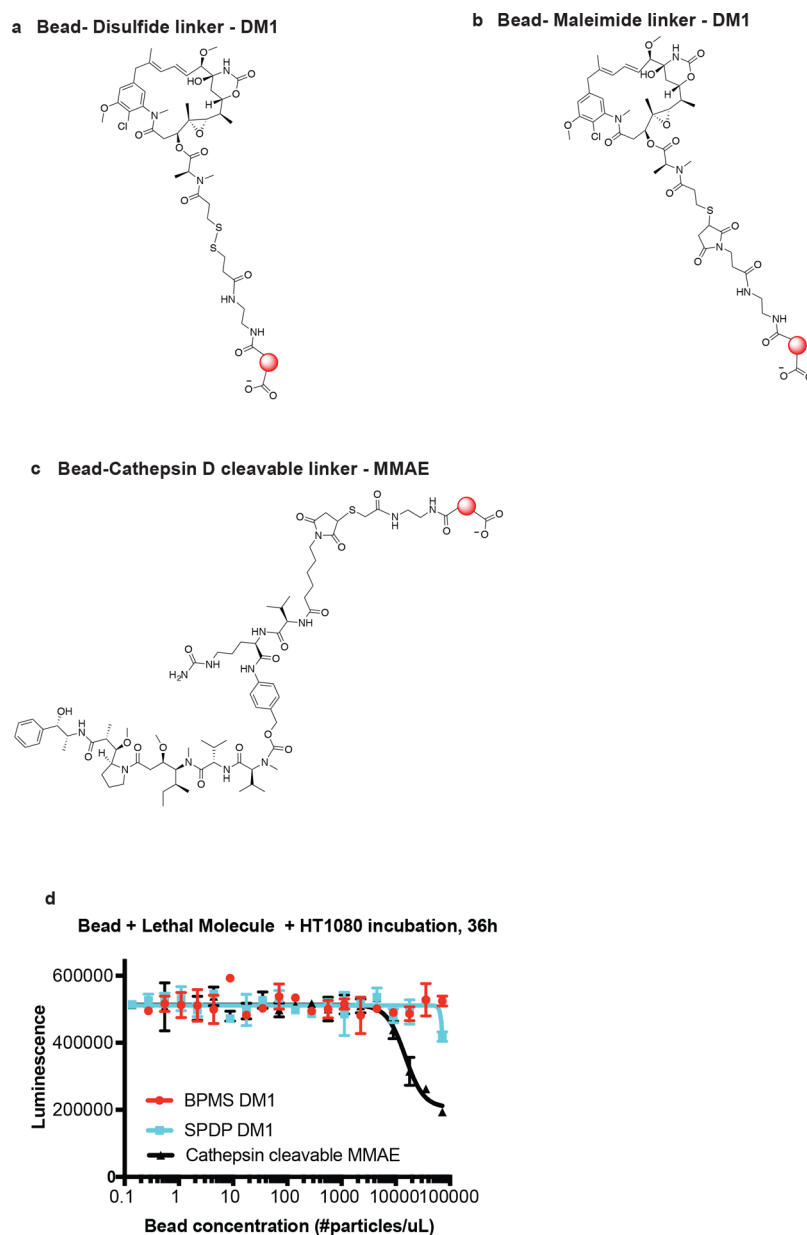


Figure 6. Small molecule component design and attachment to the bead. (a) Structure of bead–disulfide linker–DM1. (b) Structure of bead–maleimide linker–DM1. (c) Structure of bead–cathepsin D cleavable linker–monomethyl Auristatin E (MMAE). (d) Neither thiol-reduction based-cleavable nor noncleavable linkers conjugated to the beads show lethality when incubated with HT-1080 cells in varying concentrations. Cathepsin D cleavable linker-based bead system shows lethality, demonstrating effective release of MMAE upon cellular internalization.

via a cathepsin D cleavable linker (Figure 6c). After incubation of this bead system with HT-1080 cells, we observed cell lethality only when the cleavable compound was present (Supporting Information Figure 6a), suggesting that cathepsin-cleavable linkers are more effective for small molecule release, compared to disulfide linkers (Figure 6d) in the current system. Together, these constitute key elements needed for a pooled small molecule screening system, involving a solid phase system that can be taken up by cells, a cleavable linker that gets released upon cellular uptake, a fluorescent reporter that can indicate compound activity, and an amplifiable barcode that can specify compound identity.

DISCUSSION

Pooled screening of small molecules offers efficient biological evaluation of large compound libraries, and thus has distinct advantages over traditional high throughput screening methods. The potential to select small molecules that modulate biological activity through first-pass screens *in vivo* would expand current drug discovery capabilities. We examined each individual component needed for pooled, small molecule screening, whereby active small molecules could be conveniently identified based on fluorescent reporter activity.

We identified a suitable solid phase upon which to develop a small molecule delivery system for pooled screening: fluorescent silica microparticles provided enough sites for chemical diversification and maintained their inherent qualities throughout organic chemical reaction conditions. Additionally,

their fluorescence allows for easy particle tracking throughout the assay and convenient distinction from cellular debris for harvesting upon assay completion.

We designed fluorescent sensors of small molecule activity. When conjugated to beads, such sensors show a distinct signal after exposure to enzymatic activity specific to apoptotic cell death. Additionally, such sensors can likely be tuned to detect enzymatic activity of diverse peptidases.

Additionally, we established a barcode system to report on the identity of each small molecule. The barcode is compatible with deep sequencing technology, so that a statistical distribution of small molecules can be determined from the pooled assay, thus reducing the “false positive” hit molecules from the screen. The barcode does not affect the ability of the bead to be taken up by HT-1080 cells, stays with the bead throughout the duration of the assay, and can be amplified after incubation with cells undergoing death.

We initially designed this system to discover lethal small molecules that specifically initiate cell death by caspase 3. We envision that the system can be tuned and applied to wide-ranging, diverse cell models and biochemical processes as a drug and probe discovery tool. The peptide linker of the reporter can be modified to report on other proteases, protein–protein interactions, transcription, or other biological events. We tested the feasibility of doing this by changing the sensor to detect cathepsin D. Because the data suggest that this bead system is trafficked into the cell *via* endocytic pathways, the beads appear to be subject to endosomal entrapment. In addition to investigating strategies to facilitate escape from the endosome, one can use endosomal localization to detect activities in lysosomes and endosomes.

Endosomal/lysosomal targeting is one application of this technology, as there are numerous diseases associated with the disruption of lysosomal function, including Tay-Sachs disease, Gaucher’s disease, and Hurler syndrome, among others. Often, low enzymatic activity in the endosome or lysosome contributes to these disorders; this screening system enables the cell-based screening for small molecules that enhance lysosomal protease activity.

The conjugation of mertansine to the bead system requires thiol-sulfide exchange chemistry, but covalent attachment of the small molecule to the bead was effective using maleimide chemistry or NHS-reactive linkers to expand the scope of reactive moieties on the small molecule. In addition, functional handles can be broadened to include click techniques, alcohols, etc. The system can be synthesized such that a user can acquire a specific enzyme sensor/barcode/bead system and then simply conjugate to their small molecules of interest. The ability to use simple, robust bioconjugation chemistry to conjugate diverse linkers to the bead system enhances the kinds and numbers of small molecules that can be screened in this type of system.

To address applicability to a broader chemical library, we considered the usage of a self-immolative linker to attach the small molecule via the disulfide bond. After the disulfide bond is reduced, the terminal thiol can participate in a nucleophilic substitution reaction with the carbamate to form a five-membered ring; this releases the amine-containing small molecule, in its original state, without any modification. Small molecules included in the library require a reactive handle by which they are conjugated, which is a current limitation.

These studies were designed to provide an initial proof of concept. While this disulfide system was not effective at releasing compounds under the conditions we examined, it

might be possible to engineer cells to overexpress specific reductases that can cleave such a linker. We also found that a cathepsin-cleavable linker was more readily cleaved in HT-1080 cells, suggesting that this may be a simpler release mechanism. Ultimately, further optimization and diversification of the components of the system may have numerous applications in drug discovery and allow for diverse pooled small molecule screens.

METHODS

Bead Incubation with Cells. Red (540/625 nm) fluorescent, nonmagnetic, monodisperse, carboxylate coated screenCORE microspheres were purchased from Chemicell (Berlin, Product Number 6101-1). HT-1080 (fibrosarcoma) cells were obtained from American Type Culture Collection (Manassas, VA, ATCC CCL-121). HT-1080 cells were grown in DMEM high-glucose medium supplemented with 1% nonessential amino acids (Mediatech, Product Number 10-013-CM), 1% P/S, and 10% heat-inactivated fetal bovine serum (FBS). All the cell lines were grown at 37 °C under 5% CO₂ and harvested at 80% confluence for experiments. Uptake experiments were completed in six well plates (Corning costar (Corning, NY, 3516)). A total of 200 000 HT-1080 cells were plated per well and let adhere overnight at 37 °C under 5% CO₂. After 6 h of incubation with beads at 37 °C, the cells were washed twice with PBS, harvested with 0.25% Trypsin-EDTA (1X) Phenol red (Invitrogen (Carlsbad, CA, 25200-114)), resuspended in growth medium, and strained using a 70 μm filter (Fisher Scientific, 352350) into Eppendorf tubes for flow analysis.

Technology Synthesis. All chemicals were obtained from Sigma-Aldrich and used without further purification. All peptides were synthesized by LifeTein (Somerset, NJ). Oligonucleotides were synthesized by Integrated DNA Technologies (Coralville, IO). Peptide and oligonucleotide sequences are detailed in [Supporting Information Tables 1 and 2](#). This procedure was performed open to the atmosphere. Twenty-microliter beads (Chemicell (Berlin, Product Number 6101-1)) were washed with 0.1 M MES buffer (pH 6.3) by centrifugation at 14 800 rpm (16 162g) for 5 min, removing the supernatant, resuspending in a buffer, and centrifuging again. The bead pellet was resuspended in 85 μL of *N*-hydroxysulfosuccinimide sodium salt (sulfo-NHS; 20 mM in MES buffer), 8.5 μL of *N*-Boc-2,2'-(ethylenedioxy)diethylamine (50 mM, 0.5 equiv to carboxylate on bead surface), and then 42.5 μL of *N*-(3-(dimethylamino)propyl)-*N'*-ethylcarbodiimide (EDC; 100 mM in MES buffer). The reaction was stirred overnight at 37 °C before Boc-deprotection with 1000 μL of 1:1 water/trifluoroacetic acid. After 30 min, the reaction was washed six times by centrifugation and bead resuspension as described above. To the differentiated beads, 3-(2-pyridylthio)propionic acid *N*-hydroxysuccinimide ester (SPDP, 17 μM, 10 mM) was coupled by the addition of 42.5 μL of EDC (100 mM in MES buffer). The reaction was allowed to stir overnight at 37 °C before washing six times. The bead pellet was resuspended in 85 μL of *N*-hydroxysulfosuccinimide sodium salt (sulfo-NHS; 10 μM in MES buffer), 0.68 μL of peptide (5 mM, 0.001 equiv to carboxylate on bead surface), 18 μL of oligonucleotide (0.1 mM solution), and then 42.5 μL of *N*-(3-(dimethylamino)propyl)-*N'*-ethylcarbodiimide (EDC; 100 mM in MES buffer). The reaction was shaken at 37 °C overnight before washing five times with water, then four times with 0.5% Triton-X. Fluorescence of the supernatant of the final washing (494 nm excitation, 525 nm emission) was recorded to ensure there was no unconjugated fluorophore remaining with the beads. PCR reactions (procedure described below) of the final washing supernatant were completed to ensure no uncoupled barcode remained. Excess mertansine (DM1, Medchem Express, Monmouth Junction, New Jersey, serial number G01432; 10 mM in DMSO, 17 μL) was added to the bead pellet for final coupling and shaken at 37 °C overnight before washing five times with DMSO. The final system was suspended in 20 μL of DMSO (1 μL DMSO per 1 μL bead from stock solution).

Synthesis of Bead-Maleimide-DM1 Control. All chemicals were obtained from Sigma-Aldrich and used without further purification. This procedure was performed open to the atmosphere. Twenty

microliter beads (Chemicell (Berlin, Product Number 6101-1)) were washed with 0.1 M MES buffer (pH 6.3) by centrifugation at 14 800 rpm (16 162g) for 5 min, removing the supernatant, resuspending in buffer, and centrifuging again. The bead pellet was resuspended in 85 μL of *N*-hydroxysulfosuccinimide sodium salt (sulfo-NHS; 20 mM in MES buffer), 8.5 μL of *N*-Boc-2,2'-(ethylenedioxy)diethylamine (50 mM, 0.5 equiv to carboxylate on bead surface), and then 42.5 μL of *N*-(3-(dimethylamino)propyl)-*N'*-ethylcarbodiimide (EDC; 100 mM in MES buffer). The reaction was stirred overnight at 37 °C before Boc deprotection with 1000 μL of 1:1 water/trifluoroacetic acid. After 30 min, the reaction was washed six times by centrifugation and bead resuspension as described above. To the differentiated beads, *N*- β -maleimidopropyl-oxysuccinimide ester (BPMS, Thermo Fisher Scientific, Grand Island, NY, catalog number 22298, 17 μL , 10 mM) was coupled by addition of 42.5 μL of EDC (100 mM in MES buffer). The reaction was allowed to stir overnight at 37 °C before washing six times. Excess mertansine (DM1, Medchem Express, Monmouth Junction, New Jersey USA, serial number G01432; 10 mM in DMSO, 17 μL) was added to the bead pellet for final coupling and shaken at 37 °C overnight before washing five times with DMSO. The final system was suspended in 20 μL of DMSO (1 μL DMSO per 1 μL bead from stock solution).

Synthesis of Bead-Cathepsin D Cleavable Linker—Monomethyl Auristatin E. All chemicals were obtained from Sigma-Aldrich and used without further purification. This procedure was performed open to the atmosphere. Twenty microliter beads (Chemicell (Berlin, Product Number 6101-1)) were washed with 0.1 M MES buffer (pH 6.3) by centrifugation at 14 800 rpm (16 162g) for 5 min, removing the supernatant, resuspending in buffer, and centrifuging again. The bead pellet was resuspended in 85 μL of *N*-hydroxysulfosuccinimide sodium salt (sulfo-NHS; 20 mM in MES buffer), 8.5 μL of Boc-2,2'-(ethylenedioxy)diethylamine (50 mM, 0.5 equiv to carboxylate on bead surface), and then 42.5 μL of *N*-(3-(dimethylamino)propyl)-*N'*-ethylcarbodiimide (EDC; 100 mM in MES buffer). The reaction was stirred overnight at 37 °C before Boc deprotection with 1000 μL of 1:1 water/trifluoroacetic acid. After 30 min, the reaction was washed six times by centrifugation and bead resuspension as described above. The differentiated beads and 42.5 μL of EDC (100 mM in MES buffer) were added to a solution of 3-mercaptopropionic acid (17 μL , 10 mM) and 85 μL of *N*-hydroxysulfosuccinimide sodium salt (sulfo-NHS; 20 mM in MES buffer). The reaction was allowed to stir overnight at 37 °C before washing six times. The beads were resuspended in 50 μL of DMSO, and excess maleimidocaproyl-L-valine-L-citrulline-*p*-aminobenzyl alcohol *p*-nitrophenyl carbonate (MC-Val-Cit-BAP-PNP; Accela Chemicals, San Diego, California, Compound ID SY034490) was added to the reaction. The reaction was shaken at 37 °C overnight before washing five times with DMSO. To the beads was added excess monomethyl auristatin E (MMAE, Medchem Express, Monmouth Junction, New Jersey USA, catalog number HY-15162) in DMSO. The reaction was shaken at 37 °C overnight before washing five times with DMSO. Supernatant from the final wash was kept for cell viability analysis.

Bead Characterization. Microparticle size and zeta potential were measured on a Malvern Zetasizer Nano ZS (Malvern, United Kingdom). For all measurements, microparticles were diluted 1:1000 in Milli-Q water at neutral pH. The reported diameters are the average of three measurements, where each measurement comprises at least 10 acquisitions. The zeta potential was calculated according to the Smoluchowski approximation.²⁶

The absorbance of the bead-FITC-coupling reaction supernatant was measured at 494 nm to assess peptide coupling efficiency. Concentration was calculated using the Beer–Lambert law:²⁷ % coupling efficiency = $([\text{FITC reaction}] - [\text{FITC supernatant}]) / [\text{FITC reaction}] \times 100$.

Biochemical Assay for FRET Detection. A total of 0.5 units of purified, active caspase 3 protein (Abcam (Cambridge, MA, ab52101)) were incubated with 2 μL of beads in 100 μL of Apo-One buffer (Promega (Madison, WI, G7791)) for 2 h at 37 °C. The beads were

washed twice with Milli-Q water and resuspended in Milli-Q water for flow cytometry analysis.

Flow Cytometry Experiments. Flow cytometric analysis was assessed on an Accuri C6 Flow Cytometer with a 488 nm Laser. The 530/30 nm filter (FL1) was used for FITC discrimination and the 585/40 nm filter (FL2) was used for bead identification. When a live cell gate was used on DMSO treated cells, 10 000 events were recorded for each population. FACS sorting was accomplished at the Herbert Irving Comprehensive Cancer Center using a BDFacsAria II Cell Sorter.

Cell Viability Experiments. Assay plates were prepared by adding 1000 HT-1080 cells per well in 35 μL of growth media to opaque white 384 well plates (PerkinElmer (Waltham, MA, 6007688)). After adhering to the plate overnight, growth medium was removed from the cells and replaced with 35 μL of lethal molecule or beads in a 2-fold dilution series. After 24 h in the incubator, CellTiter-Glo Luminescent Cell Viability Assay (Promega (Madison, WI, G7573)) was completed. Percent viability was calculated using cell luminescence intensity values determined from a Victor 3 plate reader (PerkinElmer).

Confocal Fluorescence Imaging. Coverslips with HT-1080 cells incubated with beads (procedure described above) were washed with PBS and fixed with 4% paraformaldehyde at RT for 10 min. After 3 washes with PBS, the coverslips were mounted on slides using ProLong Diamond Antifade Mountant with DAPI (Thermo Fisher (Rochester, NY, P36966)). Confocal images were taken with a Zeiss AxioObserver LSM700 at 63 \times , and the Z Stacks were compressed with Zen software. Analysis was done using ImageJ (National Institutes of Health, Bethesda MD). All pictures are single confocal section imaged eight to 12 times to reduce noise.

Barcode Detection. Beads were exposed to 365 nm light for 10 min for PC linker cleavage. The beads were centrifuged at 14 800 rpm for 5 min, and 1 μL of the supernatant was removed for PCR amplification. Phusion Hi-Fidelity DNA polymerase (New England Biolabs) was used with primer pair CEY_Truseq_RP1: CEY_Truseq_RP1 (sequence provided in Supporting Information).

■ ASSOCIATED CONTENT

📄 Supporting Information

The Supporting Information is available free of charge on the ACS Publications website at DOI: 10.1021/acchembio.8b00043.

Supporting Figures S1–S6 and Tables S1 and S2, which show the synthetic scheme to create the delivery system, uptake analysis of beads, characterization of the C3 sensor, size analysis of beads, testing of the disulfide linker, small molecule controls, and the peptide and barcode sequences ordered (PDF)

■ AUTHOR INFORMATION

Corresponding Author

*E-mail: bstockwell@columbia.edu.

ORCID

Brent R. Stockwell: 0000-0002-3532-3868

Notes

The authors declare no competing financial interest.

■ ACKNOWLEDGMENTS

C.E.Y. was funded by the NCI Training Program in Cancer Biology Grant T32GG007284-13. The research of B.R.S. was funded by NIH/NCI (1R35CA209896 and P01CA087497).

■ REFERENCES

(1) Boutros, M., and Ahringer, J. (2008) The art and design of genetic screens: RNA interference. *Nat. Rev. Genet.* 9, 554–566.

- (2) Xing, J., Li, Q., Zhang, S., Liu, H., Zhao, L., Cheng, H., Zhang, Y., Zhou, J., and Zhang, H. (2014) Identification of dipeptidyl peptidase IV inhibitors: virtual screening, synthesis and biological evaluation. *Chem. Biol. Drug Des.* 84, 364–377.
- (3) Wan, K. H., Yu, C., George, R. A., Carlson, J. W., Hoskins, R. A., Svirskas, R., Stapleton, M., and Celniker, S. E. (2006) High-throughput plasmid cDNA library screening. *Nat. Protoc.* 1, 624–632.
- (4) Agaisse, H., Burrack, L. S., Philips, J. A., Rubin, E. J., Perrimon, N., and Higgins, D. E. (2005) Genome-wide RNAi screen for host factors required for intracellular bacterial infection. *Science* 309, 1248–1251.
- (5) Moffat, J., and Sabatini, D. M. (2006) Building mammalian signalling pathways with RNAi screens. *Nat. Rev. Mol. Cell Biol.* 7, 177–187.
- (6) Diehl, P., Tedesco, D., and Chenchik, A. (2014) Use of RNAi screens to uncover resistance mechanisms in cancer cells and identify synthetic lethal interactions. *Drug Discovery Today: Technol.* 11, 11–18.
- (7) Gargiulo, G., Serresi, M., Cesaroni, M., Hulsman, D., and van Lohuizen, M. (2014) In vivo shRNA screens in solid tumors. *Nat. Protoc.* 9, 2880–2902.
- (8) Blakely, K., Ketela, T., and Moffat, J. (2011) Pooled lentiviral shRNA screening for functional genomics in mammalian cells. *Methods Mol. Biol.* 781, 161–182.
- (9) Kainkaryam, R. M., and Woolf, P. J. (2009) Pooling in high-throughput drug screening. *Curr. Opin Drug Discov Devel* 12, 339–350.
- (10) Merrifield, R. B. (1963) Solid Phase Peptide Synthesis 0.1. Synthesis of a Tetrapeptide. *J. Am. Chem. Soc.* 85, 2149.
- (11) Barber, L. D., Bal, V., Lamb, J. R., O'Hehir, R. E., Yendle, J., Hancock, R. J., and Lechler, R. I. (1991) Contribution of T-cell receptor-contacting and peptide-binding residues of the class II molecule HLA-DR4 Dw10 to serologic and antigen-specific T-cell recognition. *Hum. Immunol.* 32, 110–118.
- (12) Furka, A., Sebestyen, F., Asgedom, M., and Dibo, G. (1991) General method for rapid synthesis of multicomponent peptide mixtures. *Int. J. Pept. Protein Res.* 37, 487–493.
- (13) Tan, D. S., Foley, M. A., Shair, M. D., and Schreiber, S. L. (1998) Stereoselective synthesis of over two million compounds having structural features both reminiscent of natural products and compatible with miniaturized cell-based assays. *J. Am. Chem. Soc.* 120, 8565–8566.
- (14) You, A. J., Jackman, R. J., Whitesides, G. M., and Schreiber, S. L. (1997) A miniaturized arrayed assay format for detecting small molecule-protein interactions in cells. *Chem. Biol.* 4, 969–975.
- (15) Chen, J. K., Lane, W. S., Brauer, A. W., Tanaka, A., and Schreiber, S. L. (1993) Biased Combinatorial Libraries - Novel Ligands for the Sh3 Domain of Phosphatidylinositol 3-Kinase. *J. Am. Chem. Soc.* 115, 12591–12592.
- (16) Poreba, M., Strozyk, A., Salvesen, G. S., and Drag, M. (2013) Caspase substrates and inhibitors. *Cold Spring Harbor Perspect. Biol.* 5, a008680.
- (17) Ginestier, C., Charafe-Jauffret, E., and Birnbaum, D. (2012) p53 and cancer stem cells: the mevalonate connexion. *Cell Cycle* 11, 2583–2584.
- (18) Edgington, L. E., Verdoes, M., and Bogyo, M. (2011) Functional imaging of proteases: recent advances in the design and application of substrate-based and activity-based probes. *Curr. Opin. Chem. Biol.* 15, 798–805.
- (19) Hengartner, M. O. (2000) The biochemistry of apoptosis. *Nature* 407, 770–776.
- (20) (2016) Venetoclax (Venclexta) for chronic lymphocytic leukemia. *Med. Lett. Drugs Ther* 58, 101–102.
- (21) Grutter, M. G. (2000) Caspases: key players in programmed cell death. *Curr. Opin. Struct. Biol.* 10, 649–655.
- (22) Seaman, J. E., Julien, O., Lee, P. S., Rettenmaier, T. J., Thomsen, N. D., and Wells, J. A. (2016) Caspases: caspases can cleave after aspartate, glutamate and phosphoserine residues. *Cell Death Differ.* 23, 1717–1726.
- (23) Dixon, S. J., Lemberg, K. M., Lamprecht, M. R., Skouta, R., Zaitsev, E. M., Gleason, C. E., Patel, D. N., Bauer, A. J., Cantley, A. M., Yang, W. S., Morrison, B., 3rd, and Stockwell, B. R. (2012) Ferroptosis: an iron-dependent form of nonapoptotic cell death. *Cell* 149, 1060–1072.
- (24) Nagy, P., Vereb, G., Damjanovich, S., Matyus, L., and Szollosi, J. (2006) Measuring FRET in flow cytometry and microscopy, *Current Protocols in Cytometry*, Chapter 12, Unit 12.18, John Wiley and Sons, Hoboken, NJ.
- (25) Kirby, B. J. (2010) *Micro- and Nanoscale Fluid Mechanics: Transport in Microfluidic Devices*, Cambridge University Press, New York.
- (26) Sze, A., Erickson, D., Ren, L., and Li, D. (2003) Zeta-potential measurement using the Smoluchowski equation and the slope of the current-time relationship in electroosmotic flow. *J. Colloid Interface Sci.* 261, 402–410.
- (27) Swinehart, D. F. (1962) The Beer-Lambert Law. *J. Chem. Educ.* 39, 333.
- (28) Talpaz, M., Shah, N. P., Kantarjian, H., Donato, N., Nicoll, J., Paquette, R., Cortes, J., O'Brien, S., Nicaise, C., Bleickardt, E., Blackwood-Chirchir, M. A., Iyer, V., Chen, T. T., Huang, F., Decillis, A. P., and Sawyers, C. L. (2006) Dasatinib in imatinib-resistant Philadelphia chromosome-positive leukemias. *N. Engl. J. Med.* 354, 2531–2541.

Toward a microparticle-based system for pooled assays of small molecules in cellular contexts

Carrie E. Yozwiak¹, Tal Hirschhorn² and Brent R. Stockwell^{1, 2,*}

¹Department of Chemistry, Columbia University, New York, NY, 10027, USA

²Department of Biological Sciences, Columbia University, Northwest Corner Building, MC 4846, 550 West 120th Street, New York, NY, 10027, USA

*Correspondence: stockwell@columbia.edu

Supporting Information

Supp Fig 1. Synthetic scheme to assemble technology.

Supp Fig 2. Cellular uptake analysis of 1 μm silica beads. (a) HT-1080 cells show uptake of polystyrene beads after 6 h incubation at 37 °C. Beads 1 μm in diameter were selected for technology development because they demonstrate sufficient cellular uptake and maximize surface area for optimal chemical conjugation. (b) 10x Microscope image of 1 μm beads incubated for 6 h in HT-1080 cells. After dilution, 9,000 beads / 200,000 HT-1080 showed uptake at a rate of one bead per one cell.

Supp Fig 3. Characterization of Bead-C3Sensor. (a) 0.1 μL of beads coupled with 0.01 equivalents FRET peptide to 1 equivalent carboxylate on the bead surface were incubated with 0.5 units active caspase 3 protein. The cleavage upon addition of active caspase 3 protein demonstrates loss of FRET. Apo-One buffer and

substrate (Promega (Madison, WI, G7791)) is used as a control (b) Zeta Potential measurement of Bead-C3Sensor system. (c) Fluorescence measurements to assess coupling efficiency of bead-FITC dual fluorescent system synthesis, Excitation = 488 nm, Emission = 525 nm for FITC detection. Bead to peptide coupling reaction shows 80% efficiency using the outlined EDC method.

Suppctfj[b]`-bZcfa Ujcb Figure 4. Dynamic light scattering experiment shows size increase upon addition of the barcode to the bead.

Gi ddcfj[b]`-bZcfa Ujcb Figure 5. Synthesis scheme to test disulfide linker cleavage.Á[
 examine disulfide bond cleavage, we have also synthesized DM1 conjugated with a non-cleavable linker, *N*-β-maleimidopropyl-oxysuccinimide ester (BPMS).

Suppctfj[b]`-bZcfa Ujcb Figure 6. Controls for small molecule component. (a) HT-1080 cells incubated for 72 h with DMSO supernatant taken from the final wash of each Bead-Lethal molecule conjugation reaction. There is no decreased cell viability observed, so cell lethality observed when the Bead-Small Molecule system is incubated with cells result exclusively from covalently linked molecules. No ambient, un-conjugated small molecules persist in a large enough concentration to confer cell death. (b) Dose response curves of HT-1080 cells with free Staurosporine, MMAE, and DM1 without bead conjugation.

Gi ddcfj[b]`-bZcfa Ujcb Table S1: Peptide sequences ordered

	Peptide Name	Sequence
Bead-FRET	CEY-FAM/DABCYL	NH2(PEG3)(fitc)KGDEVDGSGK(Dansyl)
	CEY	NH2(PEG3)(fitc)KGDEVDGSGK(Dabcyl)

	NH2DansylFITC	
	CEY_NH2_HIS	NH2-(miniPEG)3-HHHHHHHHHHHHHHHH
Bead-FITC	CEY NH2FITC	NH2(PEG3)(fitc)KGDEV
	CEY-DEVD2	NH2-(miniPEG3)-Gly-Asp-Glu-Val-Asp-Gly-Gly-Lys-(FITC)
	CEY-DEVD	NH2(mini-PEG3)-DEVD-FITC

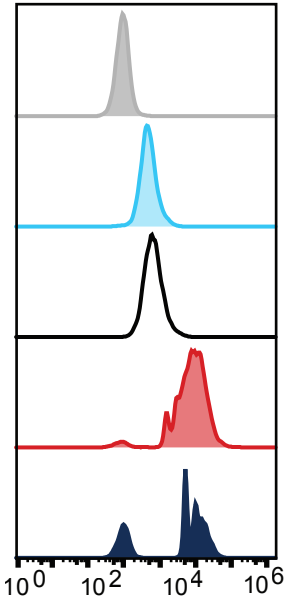
Table S2: Barcode sequences

	Sequence Name	Sequence
Bead-oligo	CEY_PCNH_rc_TruseqBC1	/5AmMC12//iSpPC/CCT TGG CAC CCG AGA ATT CCA ACG GCA TAC GAG ATC GTG ATG TGA CTG GAG TTC AGA CGT GTG CGA TCG TCG GAC TGT AGA ACT CTG AAC
Bead-oligo	CEY_PCNH_TruseqBC2	/5AmMC12//iSpPC/GTT CAG AGT TCT ACA GTC CGA CTG AAC TCC AGT CAC CGA TGT ATC TCG TAT GCC GTC TTC TGC ACA TTG TGG AAT TCT CGG GTG CCA AGG
control	CEY_Truseq_BC2_PAGE	GTT CAG AGT TCT ACA GTC CGA CTG AAC TCC AGT CAC CGA TGT ATC TCG TAT GCC GTC TTC TGC ACA TTG TGG AAT TCT CGG GTG CCA AGG
control	CEY_TruseqBC1	GTT CAG AGT TCT ACA GTC CGA CGA TCG CAC ACG TCT GAA CTC CAG TCA CAT CAC GAT CTC GTA TGC CGT TGG AAT TCT CGG GTG CCA AGG

control	CEY_TrueSeqBC1_revcomp	CCT TGG CAC CCG AGA ATT CCA ACG GCA TAC GAG ATC GTG ATG TGA CTG GAG TTC AGA CGT GTG CGA TCG TCG GAC TGT AGA ACT CTG AAC
control	CEY_NH_TrueSeqBC1	/5AmMC12/GTT CAG AGT TCT ACA GTC CGA CGA TCG CAC ACG TCT GAA CTC CAG TCA CAT CAC GAT CTC GTA TGC CGT TGG AAT TCT CGG GTG CCA AGG
Primer 1	CEY_TrueSeq_RP11	CAA GCA GAA GAC GGC ATA CGA GAT CGT GAT GTG ACT GGA GTT CCT TGG CAC CCG AGA ATT CCA
Primer 2	CEY_TrueSeq_RP1	AAT GAT ACG GCG ACC ACC GAG ATC TAC ACG TTC AGA GTT CTA CAG TCC GA

Supporting Information Figure 2

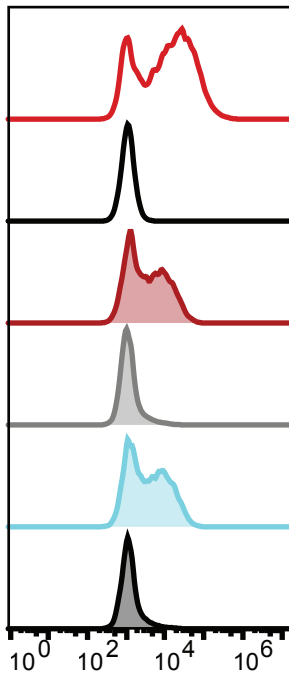
a Different Diameter Beads incubated with HT-1080 Cells, 6 h



585 Fluorescence Emission Intensity

- HT-1080 cells
- 0.1 μm Beads + HT-1080 cells
- 0.2 μm Beads + HT-1080 cells
- 1 μm Beads + HT-1080 cells
- 2 μm Beads + HT-1080 cells

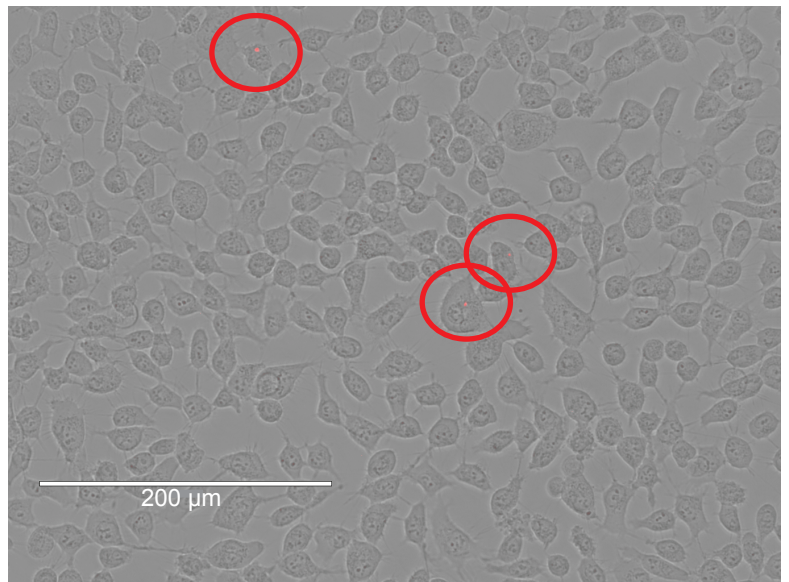
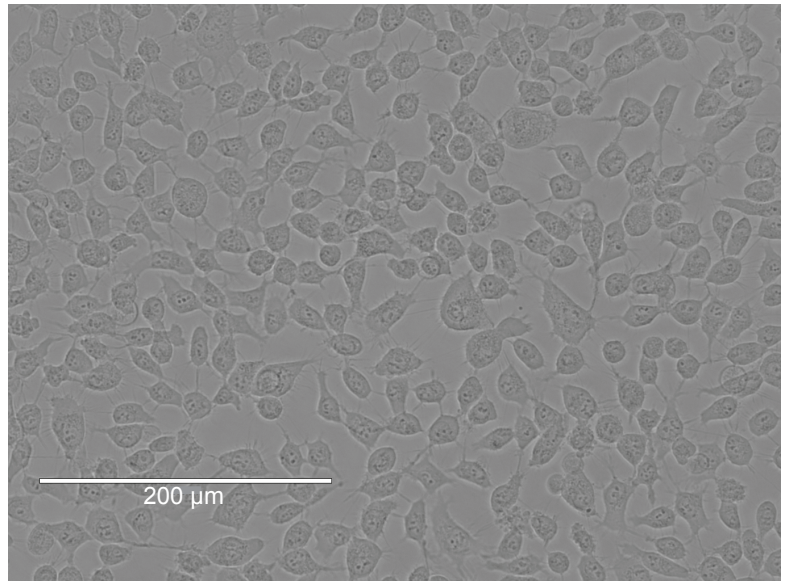
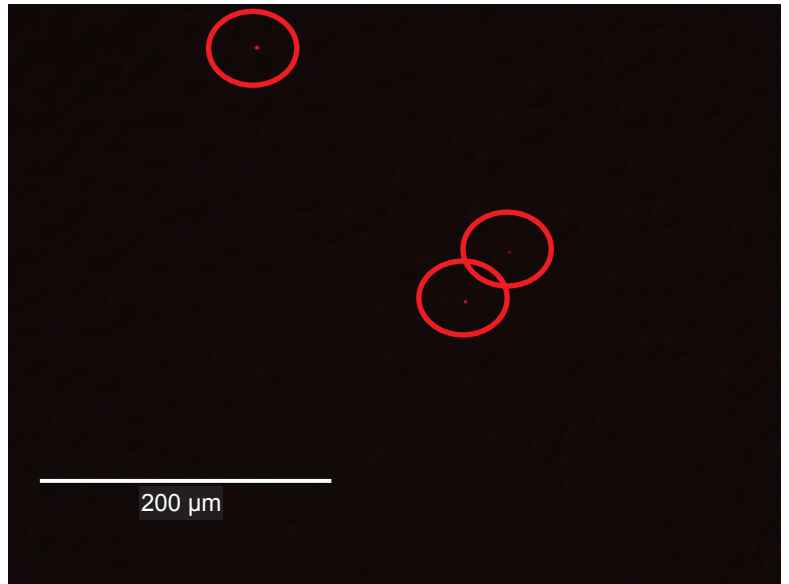
c 1 μm Silica beads incubated with different cell lines, 14 h



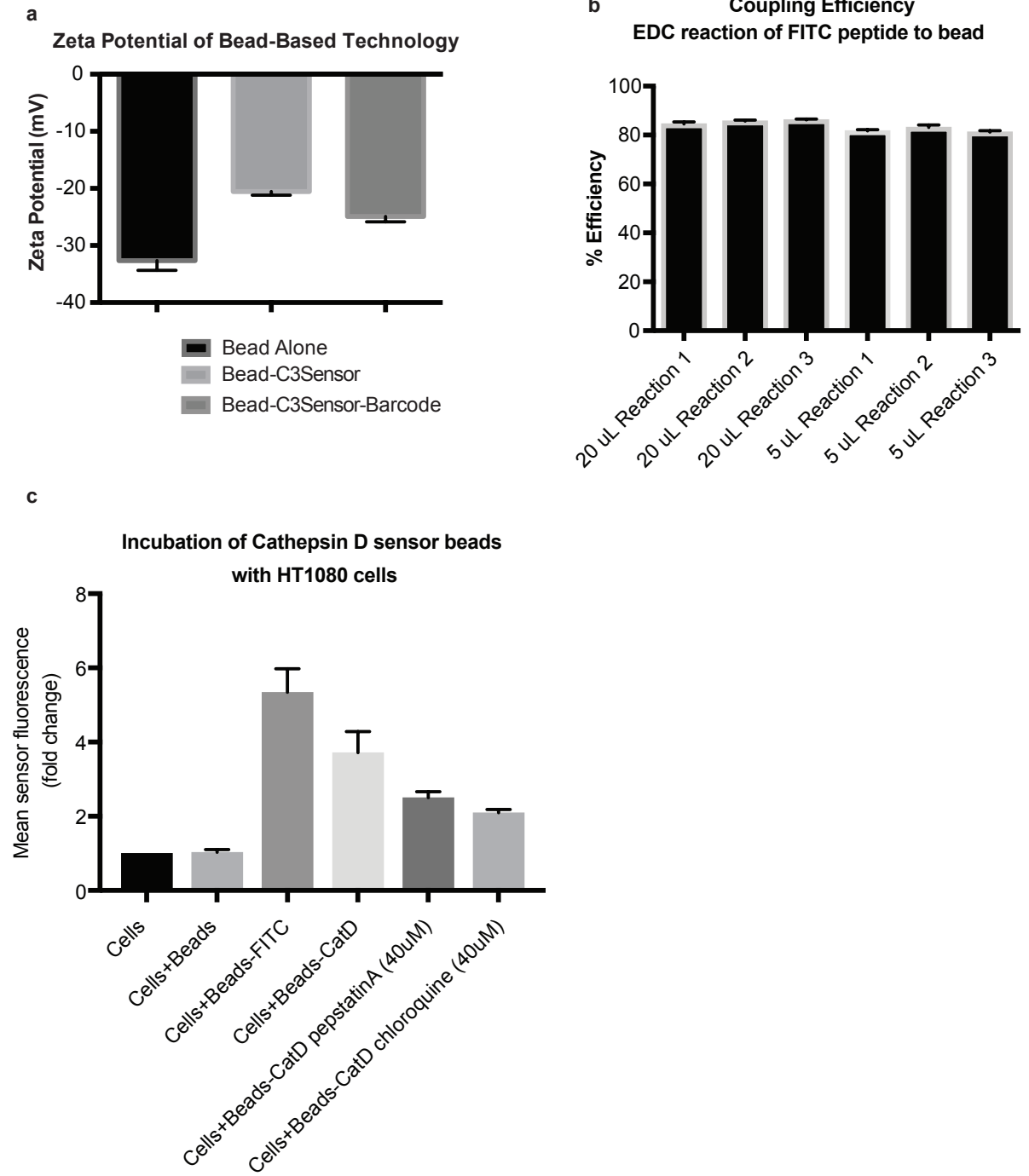
585 Fluorescence Emission Intensity

- 1 μm Beads + HT-1080 cells
- HT-1080 Cells
- 1 μm Beads + 293-T cells
- 293-T Cells
- 1 μm Beads + RKN cells
- RKN Cells

b Images of uptake, MOI dilution for 1 bead/cell
10x Magnification

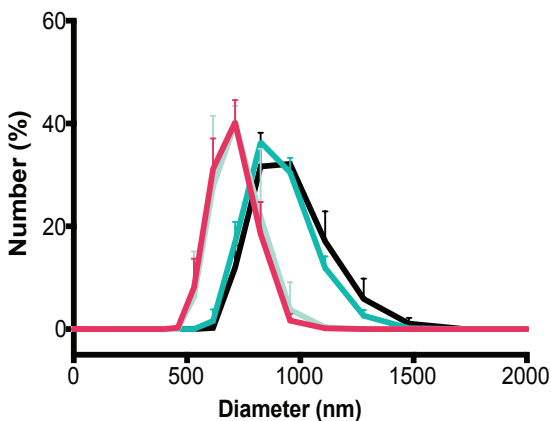


Supporting Information Figure 3



Supporting Information Figure 4

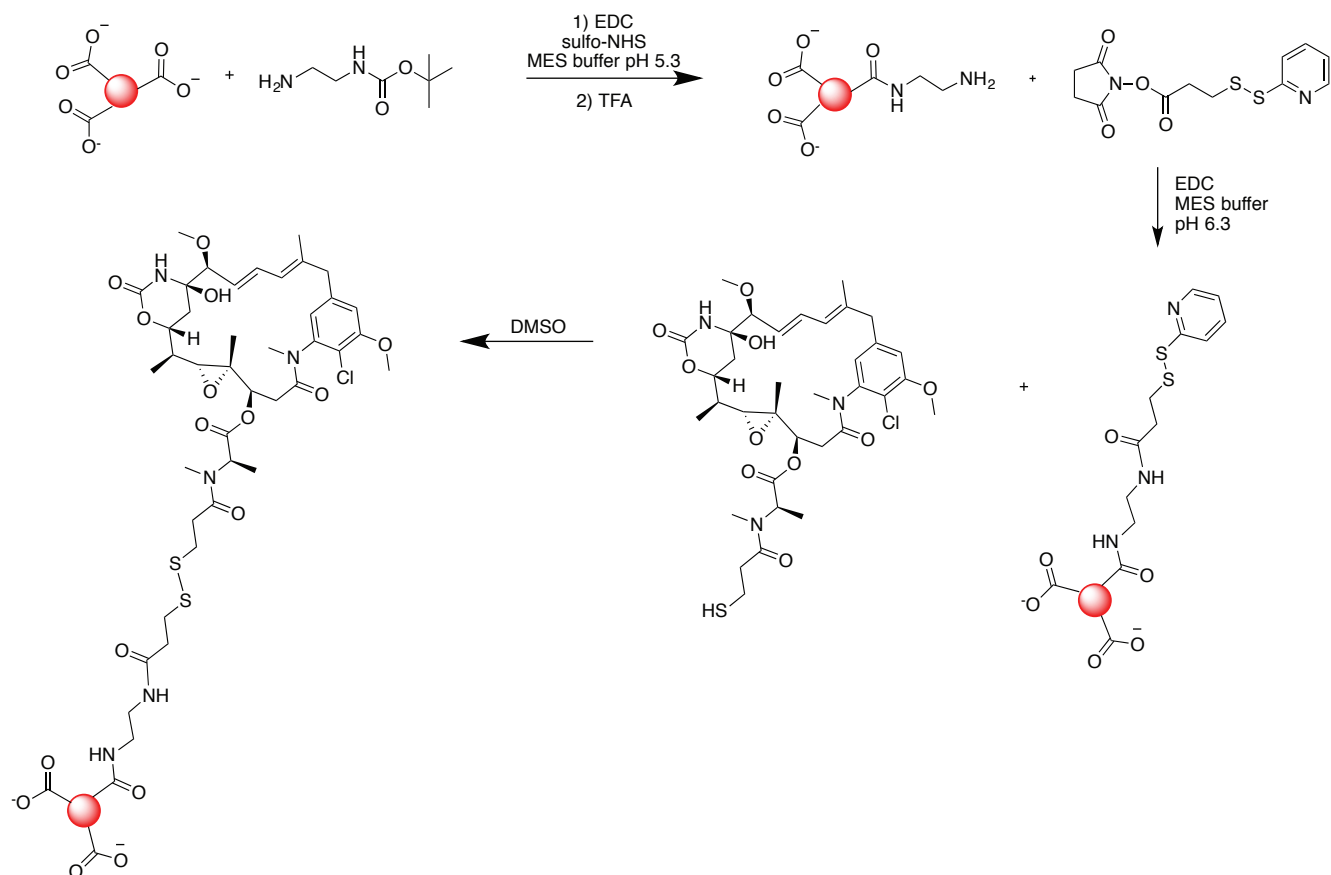
Dynamic Light Scattering



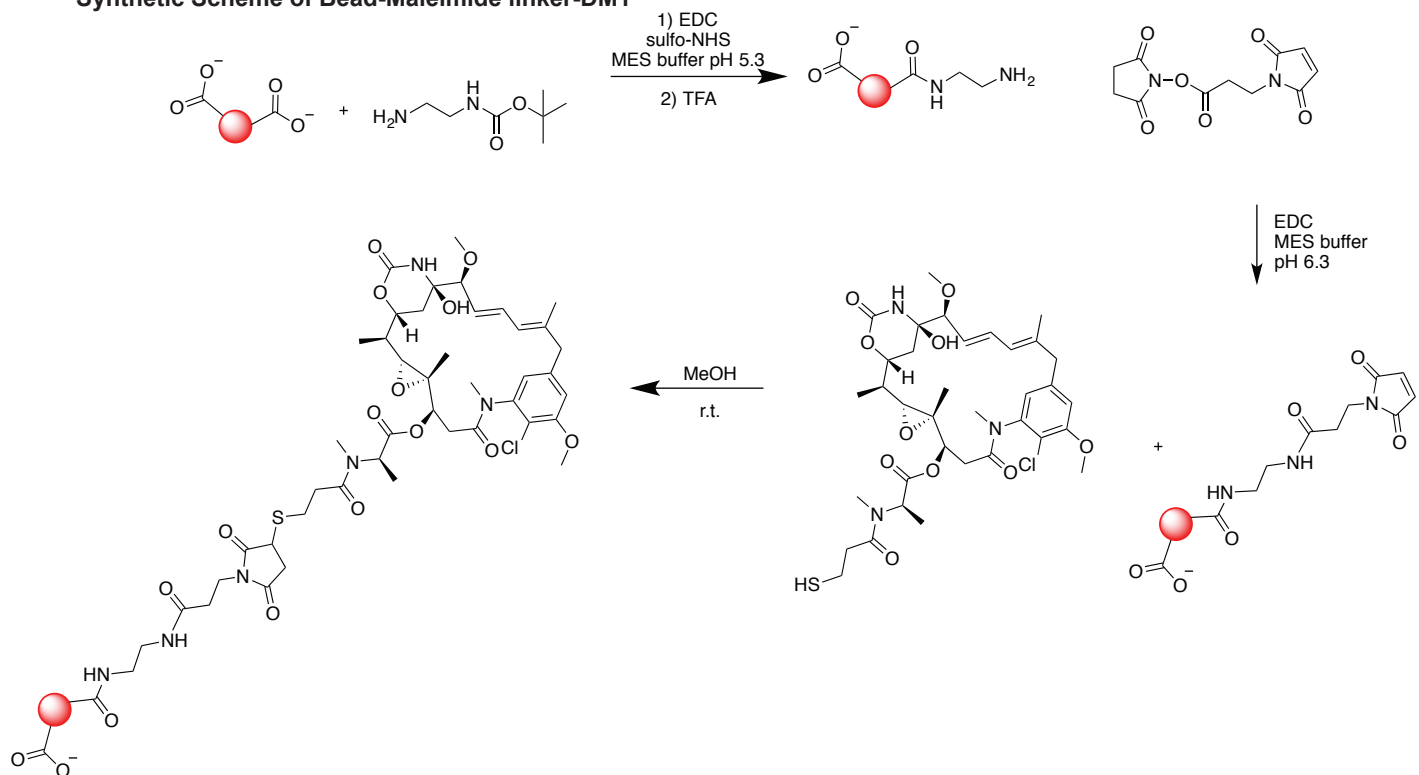
- Beads alone
- Beads-C3Sensor
- Beads-C3Sensor-Barcode 1
- Beads-C3Sensor-Barcode 2

Supporting Information Figure 5

a Synthetic Scheme of Bead-Disulfide linker-DM1



b Synthetic Scheme of Bead-Maleimide linker-DM1



Supporting Information Figure 6

